

Inorganic Chemistry

Optically Visible Phase Separation between Mott-Hubbard and Charge-Density-Wave Domains in a Pd-Br Chain Complex

Takefumi Yoshida,^[a] Shinya Takaishi,^{*[a]} Hiroaki Iguchi,^[a] Hiroshi Okamoto,^[b] Hisaaki Tanaka,^[c] Shin-ichi Kuroda,^[c] Yuka Hosomi,^[d] Shoji Yoshida,^[d] Hidemi Shigekawa,^[d] Tatsuhiro Kojima,^[e] Hiroyoshi Ohtsu,^[e] Masaki Kawano,^[e] Brian K. Breedlove,^[a] Laurent Guérin,^[f] and Masahiro Yamashita^{*[a]}

We synthesized a bromo-bridged Pd complex, which underwent as lowering the temperature a charge-density-wave (CDW) to Mott-Hubbard (MH) phase transition, as confirmed by using X-ray diffraction analysis, ESR, FT-IR and Raman spectroscopies. The complex showed a phase-separation phenomenon with a striped pattern over a wide temperature range, and domain propagation was observed using an optical microscope. Moreover, we observed changes in the local electronic state accompanying the phase transition by using scanning tunneling microscopy (STM)

Charge bistability in solid-state complexes is a key property for functional materials. There has been great effort put into switching the properties, such as charge-transfer phase transitions (CTPT), by using optical,^[1] thermal,^[2] and electrical^[3] stimuli. However, there are still many challenges in designing materials which undergo CTPT by controlling molecular charge

bistability and its cooperativity. Quasi-one-dimensional halogen-bridged metal complexes are good candidates for these types of materials because they possess charge bistability based on the oxidation states of the metal ions as well as highly isolated one-dimensional (1D) electronic system composed of d_z^2 orbital of metal ions (M) and p_z orbital of bridging halide ions (X). In other words, they can exhibit averaged valence Mott-Hubbard (MH) and mixed valence charge-density-wave (CDW) states. Ni complexes are primarily in an MH state with a $-X-M^{III}-X-M^{III}-X-$ linear chain structure, in which bridging halides locate at the midpoint between the neighboring metal ions,^[4] thus they are classified as Robin-Day class III complexes.^[5] They show marked physical properties due to strong electron correlation of the Ni^{III} states.^[6] On the other hand, Pd and Pt complexes are known to be in a CDW state ($-X-M^{II}-X-M^{IV}-X-$), in which bridging halides displaced from the midpoint, and are classified Robin-Day class II type complexes.^[5] They show characteristic mixed valence state properties, such as luminescence with large Stokes shifts,^[7] overtone progressions in the resonant Raman spectra,^[8] and intervalence charge transfer transitions.^[9] Although over 300 complexes have so far been reported since Wolfram reported the first chloro-bridged Pt complex in 1990,^[10] no exceptions were reported before our recent research.

Recently, we have reported the first example of a Pd complex, $[Pd(en)_2Br](C_5-Y)_2 \cdot H_2O$ (en = ethylenediamine; C_5-Y = dipentylsulfocuccinate), exhibiting CTPT between CDW and MH states at 205 K.^[11] This CTPT was related to large temperature dependence in Pd...Pd distance (from 5.31 Å (300 K) to 5.21 Å (100 K)). The Pd^{III} MH state was shown to be stabilized by short Pd...Pd distance and resultant single well potential of the bridging Br⁻ ion (Figure 1(b)).^[11c] The CTPT was classified into the first-order transition with a hysteresis, because this phase transition is accompanied by large structural change (e.g. Pd...Pd distance jumps by ca. 0.03 Å). This is probably because the phase transition is coupled with the alkyl chain dynamics. One of our goals is to explore the boundary region between CDW state with double well potential (Figure 1a) and MH state with single well potential (Figure 1b). From this point of view, $[Pd(en)_2Br](C_5-Y)_2 \cdot H_2O$ is not suitable because the first order phase transition is accompanied by large structural change with the formation of a 3D ordering of the CDW state, there-

[a] T. Yoshida, Dr. S. Takaishi, Dr. H. Iguchi, Dr. B. K. Breedlove, Prof. M. Yamashita
Department of Chemistry, Graduate School of Science, Tohoku University, 6-3 Aza-aoba, Aramaki, Sendai 980-8578, Japan
and
WPI-Advanced Institute for Materials Research, Tohoku University, 2-1-1 Katahira, Sendai 980-8577, Japan
E-mail: takaishi@mail.tains.tohoku.ac.jp
yamashita@agnus.chem.tohoku.ac.jp

[b] Prof. H. Okamoto
Department of Advanced Materials Science, Graduate School of Frontier Sciences, The University of Tokyo, Kashiwa 277-8561, Japan

[c] Dr. H. Tanaka, Prof. S.-i. Kuroda
Department of Applied Physics, Graduate School of Engineering, Nagoya University, Furocho, Chikusa-ku, Nagoya 464-8603, Japan

[d] Y. Hosomi, Dr. S. Yoshida, Prof. H. Shigekawa
Faculty of Pure and Applied Sciences, University of Tsukuba, Tsukuba 305-8573, Japan

[e] Dr. T. Kojima, Dr. H. Ohtsu, Prof. M. Kawano
Division of Advanced Materials Science, Pohang University of Science and Technology (POSTECH), RIST Building 3-3390, 77 Cheongam-Ro, Nam-Gu, Pohang, Gyeongbuk 790-784, South Korea

[f] Dr. L. Guérin
Université de Rennes 1, Institut de Physique de Rennes, 263 Av. du Général Leclerc, 35042 Rennes cedex, France

Supporting Information for this article is available on the WWW under <http://dx.doi.org/10.1002/slct.201600065>

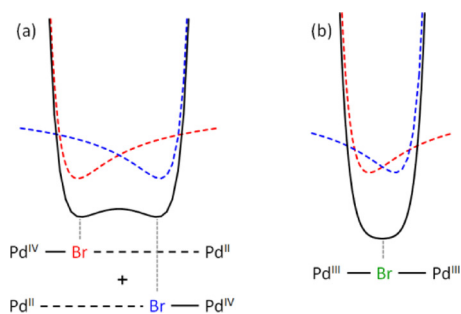


Figure 1. Schematic illustration of potential curve of bridging Br^- ions in (a) a CDW state and (b) an MH state. Blue and red dotted lines represent the potential curves attributable to $\text{Pd}^{\text{IV}}\text{-Br}$ or $\text{Pd}^{\text{II}}\text{-Br}$ sub-structures. Black solid lines express the potential curves of Pd-Br-Pd structure (sum of the red and blue dotted lines).

fore limiting the domain of coexistence of the two phases. In order to explore the boundary region, in this work, we developed a new bromo-bridged Pd complex, $[\text{Pd}(\text{cptn})_2\text{Br}]\text{Br}_2$ (**1**), ($\text{cptn} = 1R,2R$ -diaminocyclopentane) without alkyl chains to make crystalline lattice rigid, which could afford less structural difference between two phases. We found that **1** showed a very peculiar CDW-MH CTPT as well as coexistence of both phases in a single crystal with a stripe patterned phase separation over a wide temperature range, which could be observed with an optical microscope. Here we report its crystal structure, its physical properties including the phase separation phenomenon and the local electronic state visualized by STM.

The crystal structure and crystallographic data of **1** at 93 K are shown in Figure 2 and Table S1, respectively. CCDC 1449578 contains the supplementary crystallographic data of **1**. For comparison, we re-analyzed the crystal structure of $[\text{Pd}(\text{chxn})_2\text{Br}]\text{Br}_2$ ($\text{chxn} = 1R,2R$ -diaminocyclohexane), which has reported to be in a CDW state,^[12] at 93 K. The Pd ion was found to have an elongated octahedral geometry. Square planar $\text{Pd}(\text{cptn})_2$ moieties are bridged by Br^- anions, forming a linear chain along a -axis. These linear chains and free Br^- counteranions are connected by $\text{N-H}\cdots\text{Br}\cdots\text{H-N}$ hydrogen bonds along b -axis to form a two-dimensional sheet (Figure 2a). On the other hand, there are no chemical bonds other than van der Waals interaction between the sheets (Figure 2c). The structural features of **1**, including space group ($I222$), are similar to those of $[\text{Pd}(\text{chxn})_2\text{Br}]\text{Br}_2$. However, there are several subtle differences as described below. First, the $\text{Pd}\cdots\text{Pd}$ distances along the 1D chain (5.2223(4) Å at 93 K) are slightly shorter than those of $[\text{Pd}(\text{chxn})_2\text{Br}]\text{Br}_2$ (5.2784(4) Å at 93 K). Temperature dependency of $\text{Pd}\cdots\text{Pd}$ distances in both compounds are plotted in Figure S1. In a previous report, we have proposed that the $\text{Pd}\cdots\text{Pd}$ distances are important for determining the electronic state of the Pd complexes. In the case of bromo-bridged Pd complexes, we have proposed that MH and CDW states occur when the $\text{Pd}\cdots\text{Pd}$ distances are shorter and longer than ca. 5.26 Å, respectively. In fact, $[\text{Pd}(\text{chxn})_2\text{Br}]\text{Br}_2$ with longer $\text{Pd}\cdots\text{Pd}$ distances than 5.26 Å is known to have CDW state at any temperature. On the other hand, $\text{Pd}\cdots\text{Pd}$ distances of **1** at 93 K is shorter than the boundary distance. Thus, we expected that **1** is in an MH state at

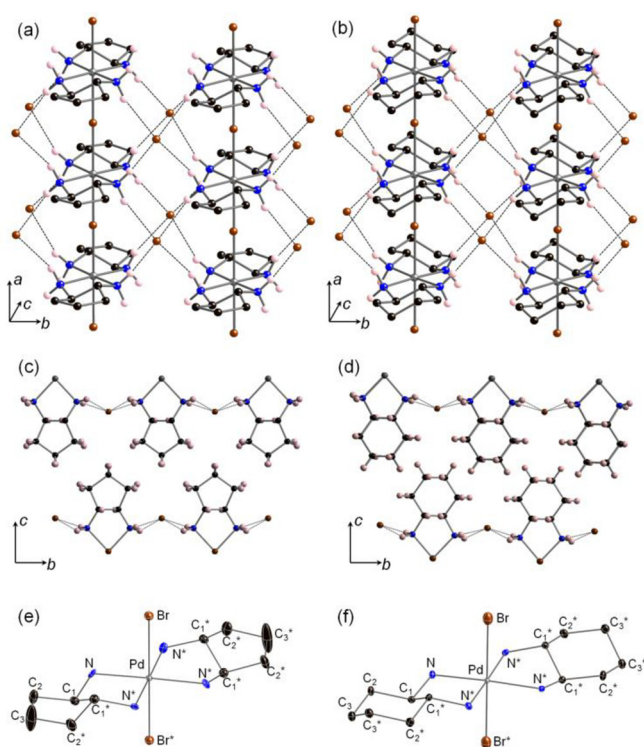


Figure 2. Perspective views of the crystal packings along c -axis (a and b) and a -axis (c and d), and ORTEP drawings with thermal ellipsoids at 50% probability in **1** and $[\text{Pd}(\text{chxn})_2\text{Br}]\text{Br}_2$, respectively ($T = 93$ K). Gray; Pd, brown; Br, blue; N, black; C, pink; H, Hydrogen atoms are partly omitted for clarity.

this temperature. The subtle difference (ca. 0.05 Å) in $\text{Pd}\cdots\text{Pd}$ distances between the two compounds could be because cycloalkane rings existing between the 2D sheets in $[\text{Pd}(\text{chxn})_2\text{Br}]\text{Br}_2$ sterically more crowded compared to **1** (Figure 2c and d), that makes $\text{Pd}\cdots\text{Pd}$ distances longer. Hirshfeld surface and fingerprint plots^[13] for $\text{H}\cdots\text{H}$ contact of **1** and $[\text{Pd}(\text{chxn})_2\text{Br}]\text{Br}_2$ (Figure S2) suggested that **1** has weaker intermolecular $\text{H}\cdots\text{H}$ contacts than $[\text{Pd}(\text{chxn})_2\text{Br}]\text{Br}_2$ (less red area). This finding supports the aforementioned hypothesis. Second, the thermal ellipsoids of the bridging halides of $[\text{Pd}(\text{chxn})_2\text{Br}]\text{Br}_2$ were elongated along the a -axis, whereas those of **1** were mostly spherical. The elongated thermal ellipsoids correspond to a disordered atom at the displaced position from the midpoint due to the double well potential. Thus, the spherical ones suggest that **1** is in an MH state at this T . The actual electronic state cannot be determined by conventional X-ray crystal structure analysis. Third, the thermal ellipsoid of C_3 in the cptn ligand is exceptionally large due to a flipping motion of the C_3 atom. However, the relationship between this flipping motion and electronic state of **1** has not yet been determined.

In order to determine the electronic states of **1** at various T , we acquired X-ray diffraction (XRD) photographs (Figure S3). At 220 K, we observed diffuse peaks at $h = m + 1/2$ (m is an integer), which correspond to a cell doubling along the chain associated to the CDW state. These superlattice peaks were found to be rod-shaped diffuse scatterings from the reconstructed diffraction image of the reciprocal lattice (Figure S3). These diffuse scatterings are due to the long range cor-

relation of CDW phase along *a* and *b*-axis and very small correlation along *c*-axis. Therefore, the structural state of **1** at 220 K consists of a stacking of almost uncorrelated 2D CDW long range order sheets. The intensity of the diffuse scatterings gradually weakened upon cooling and mostly disappeared at 100 K, indicating that the electronic state of **1** is changing from CDW to MH state gradually. This is in contrast to the case of $[\text{Pd}(\text{en})_2\text{Br}](\text{C}_5\text{-Y})\cdot\text{H}_2\text{O}$, which showed abrupt transition from the 3D CDW to the MH state signed by the disappearance of the superlattice Bragg peaks at $T_c = 205$ K.^[11a] In the spin susceptibility measurements, phase transition phenomena between diamagnetic CDW state and paramagnetic MH state was observed but its change is very gradual compared to $[\text{Pd}(\text{en})_2\text{Br}](\text{C}_5\text{-Y})\cdot\text{H}_2\text{O}$ (see Figure S4). Once again, this gradual change of the spin susceptibility in **1** can be explained by the 2D character of the transition as opposed to the 3D ordering of the CDW state in $[\text{Pd}(\text{en})_2\text{Br}](\text{C}_5\text{-Y})\cdot\text{H}_2\text{O}$.

Optical images of a single crystal of **1** at various *T* are shown in Figure 3 and S5. This sample had a reddish luster at

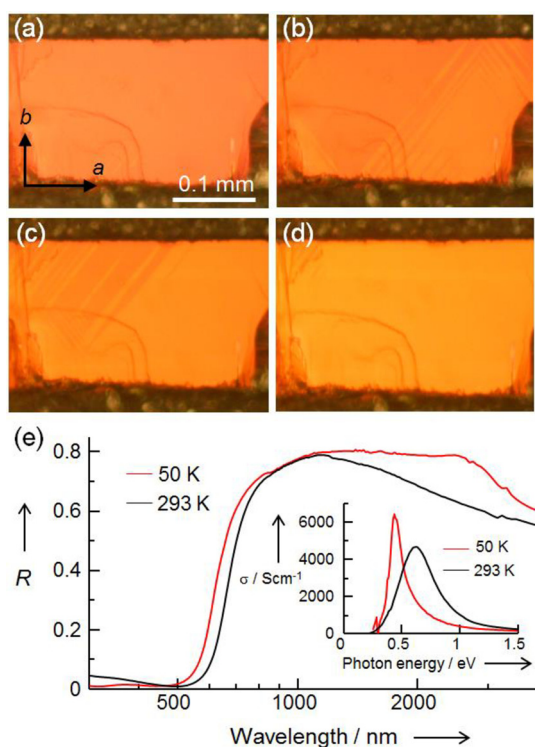


Figure 3. Optical images of the single crystal of **1** at (a) 130 K, (b) 120 K, (c) 100 K and (d) 50 K, and (e) optical reflectivity spectra (*E* // chain). Inset shows optical conductivity spectra of **1** obtained by Kramers-Kronig transformation of the optical reflectivity spectra.

room *T*. The color did not change even after cooling to 130 K (Figure 3(a)). Below 130 K, on the other hand, a yellowish domain appeared and showed a striped pattern parallel to the (1 1 0) or (−1 1 0) directions. At 50 K, most of the crystal had a yellowish luster. Although texture of domain propagation depended on the sample batches, the change in color could be repeated with the same crystal by cooling and heating. This re-

sult clearly indicates that some phase separation is occurring in **1** in a wide *T* range.

In order to determine the electronic state of each domain, we acquired Raman spectra of **1** at various *T* using Raman microscope (beam size ≈ 1 μm). It has been established that Br–Pd–Br symmetrical stretching mode is Raman active and observed at around 130 cm^{-1} in CDW states,^[11a] whereas it is inactive in MH states. As shown in Figure 4, clear Raman peaks

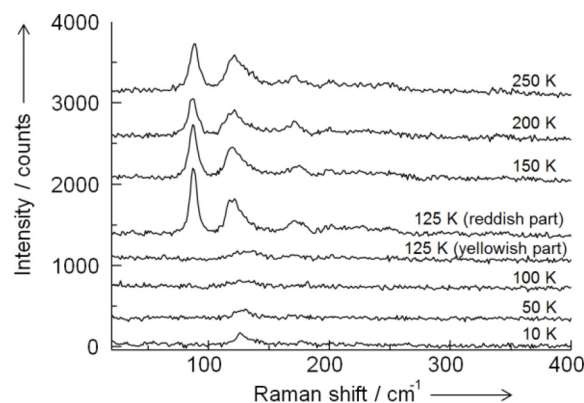


Figure 4. Raman spectra of **1** at various *T*.

were observed at ~ 90 and 130 cm^{-1} above 150 K. On the basis of a previous study, we assigned the latter peak to the Br–Pd–Br symmetrical stretching mode, although the former could not be assigned at present. Below 100 K, both peaks disappeared. In other words, **1** underwent a phase transition to an MH state below 100 K. At 125 K, Raman spectra for the reddish and yellowish domains were acquired. For the reddish domain, a spectrum was characteristic of high temperature (CDW) phase, whereas the spectrum for the yellowish domain was corresponding to an MH state. Thus, we concluded **1** showed phase separation phenomenon between CDW and MH phases at wide *T* range.

Besides XRD and Raman spectroscopy, FT-IR spectroscopy can be used to determine the electronic state of MX complexes because the N–H symmetrical stretching mode ($\nu(\text{NH})$) shows single peak in an MH state and double peaks in a CDW state.^[14] We measured the FT-IR spectra of a single crystal of **1** using an FT-IR microscope (aperture size = 130×130 μm) at 100 K where the phase separation occurs. FT-IR spectra of single crystal at different position (area 1 and area 2 in inset of Figure 5) of **1** at 100 K are shown in Figure 5. As can be seen, area 1 is mostly composed of yellowish domain whereas area 2 is mostly composed of reddish domain. The FT-IR spectra showed single and double peak at $\nu(\text{NH})$ region at area 1 and area 2, respectively. This result is another evidence of the charge separation phenomenon between CDW and MH domains.

STM is a powerful technique for visualizing the local electronic structure. In the previous paper, we have reported the STM image for isostructural $[\text{M}(\text{chxn})_2\text{Br}]\text{Br}_2$ (*M* = Ni and Pd).^[15] Ni and Pd compounds afforded bright spots approximately every 5 Å and 10 Å along the chain, respectively, which reflects the periodicity of the charge arrangements in MH and CDW

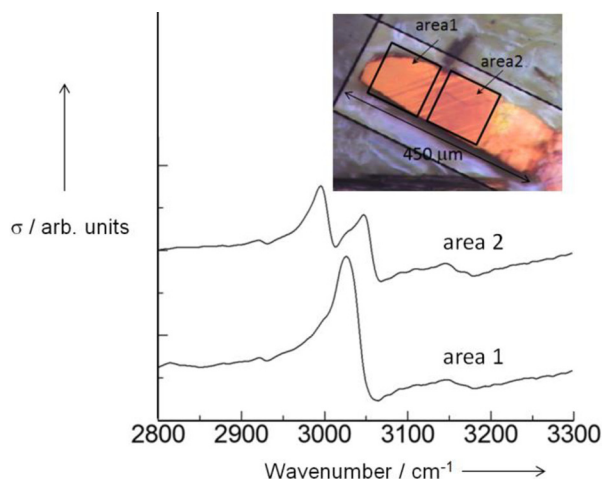


Figure 5. FT-IR spectra ($E \perp$ chain) on the different sample position at 100 K.

states. In this study, we cleaved the single crystal of **1** using adhesive tape so as to expose flat surface of ab plane after mounted to the sample stage with carbon paste. STM images of **1** in the ab plane are shown in Figure 6. At 114 K, bright spots were observed approximately every 10 Å along the chain, indicating that **1** was in a CDW state at this T . At 106 K, on the other hand, the bright spots were observed approximately every ~ 5 Å along the chain, confirming that **1** was in an MH state at this T . Because these images were acquired with positive sample bias, bright spots represent tunnel current from the Fermi energy of the tip to the conduction band of the sample, which are the upper Hubbard d_z^2 band of Pd^{3+} for MH state and d_z^2 band of Pd^{4+} for CDW state. To the best of our knowledge, this is the first observation of a change in the local electronic state with molecular spatial resolution, accompanied by a CTPT, using STM.

In conclusion, we synthesized the bromo-bridged Pd complex $[\text{Pd}(\text{cptn})_2\text{Br}]\text{Br}_2$. This complex showed CDW-to-MH CTPT accompanied by phase separation phenomena over a wide temperature range, which was confirmed by using X-ray diffraction, ESR, Raman, optical reflectivity, and FT-IR spectroscopies. In addition, we determined the local electronic state by using temperature-dependent STM. To the best of our knowledge, this is the first observation to detect the change in local electronic state accompanied by a CTPT with molecular spatial resolution. The mechanism for the phase separation phenomenon is currently under investigation.

Supporting Information

Experimental Section, Crystallographic parameters (Table S1), Temperature dependence of Pd–Pd distance (Figure S1), Hirshfeld surface plots (Figure S2), X-ray reconstructed photographs (Figure S3), ESR spectra (Figure S4), and optical images (Figure S5) of **1**.

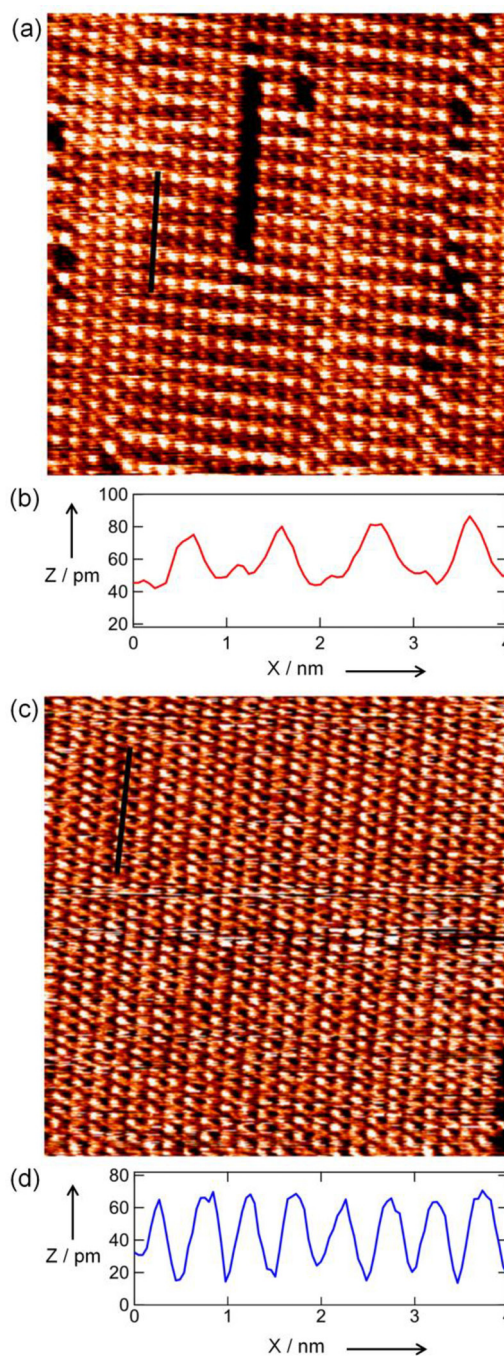


Figure 6. STM topographic images of **1** at (a) 114 K and (c) 106 K. (b) and (d) show height profiles on the black lines drawn on the images (a) and (c), respectively.

Acknowledgements

This work was partly supported by a JSPS KAKENHI grant (A) 26248015, a Grant-in-Aid for Young Scientist (B) 25810032, and CREST, JST.

Keywords: charge-transfer phase transition • phase separation • local electronic states • charge bistability • quasi-one-dimensional halogen-bridged metal complex

- [1] a) S. Koshihara, Y. Tokura, T. Mitani, G. Saito, T. Koda, *Phys. Rev. B* **1990**, *42*, 6853–6856; b) S. Iwai, M. Ono, A. Maeda, H. Matsuzaki, H. Kishida, H. Okamoto, Y. Tokura, *Phys. Rev. Lett.* **2003**, *91*, 057401; c) H. Uemura, H. Okamoto, *Phys. Rev. Lett.* **2010**, *105*, 258302; d) Y. Tokura, *J. Phys. Soc. Jpn.* **2006**, *75*, 011001; e) H. Ichikawa, S. Nozawa, T. Sato, A. Tomita, K. Ichiyonagi, M. Chollet, L. Guerin, N. Dean, A. Cavalleri, S. Adachi, T. H. Arima, H. Sawa, Y. Ogimoto, M. Nakamura, R. Tamaki, K. Miyano, S. Y. Koshihara, *Nature Mater.* **2011**, *10*, 101–105. f) M. Dressel, *Naturwissenschaften* **2007**, *94*, 527–541.
- [2] a) J. B. Torrance, A. Girlando, J. J. Mayerle, J. I. Crowley, V. Y. Lee, P. Batail, *Phys. Rev. Lett.* **1981**, *47*, 1747–1750. b) J. B. Torrance, A. Girlando, J. J. Mayerle, J. I. Crowley, V. Y. Lee, P. Batail, *Phys. Rev. Lett.* **1981**, *47*, 1747–1750. c) J. B. Torrance, J. E. Vazquez, J. J. Mayerle, V. Y. Lee, *Phys. Rev. Lett.* **1981**, *46*, 253–257; d) Y. Iwasa, T. Koda, Y. Tokura, A. Kobayashi, N. Iwasawa, G. Saito, *Phys. Rev. B* **1990**, *42*, 2374–2377; e) H. Tokoro, S.-i. Ohkoshi, T. Matsuda, K. Hashimoto, *Inorg. Chem.* **2004**, *43*, 5231–5236; f) H. Kitagawa, N. Onodera, T. Sonoyama, M. Yamamoto, T. Fukawa, T. Mitani, M. Seto, Y. Maeda, *J. Am. Chem. Soc.* **1999**, *121*, 10068–10080; g) N. Kojima, W. Aoki, M. Itoi, M. Seto, Y. Kobayashi, Y. Maeda, *Solid State Commun.* **2001**, *120*, 165–170.
- [3] a) Y. Iwasa, T. Koda, S. Koshihara, Y. Tokura, N. Iwasawa, G. Saito, *Phys. Rev. B* **1989**, *39*, 10441–10444; b) R. Kumai, Y. Okimoto, Y. Tokura, *Science*, **1999**, *284*, 1645–1647; c) F. Sawano, I. Terasaki, H. Mori, T. Mori, M. Watanabe, N. Ikeda, Y. Nogami, Y. Noda, *Nature* **2005**, *437*, 522–524.
- [4] K. Toriumi, Y. Wada, T. Mitani, S. Bandow, M. Yamashita, Y. Fujii, *J. Am. Chem. Soc.* **1989**, *111*, 2341–2342.
- [5] M. B. Robin, P. Day, *Adv. Inorg. Radiochem.* **1967**, *10*, 247–422.
- [6] a) H. Kishida, H. Matsuzaki, H. Okamoto, T. Manabe, M. Yamashita, Y. Taguchi, Y. Tokura, *Nature* **2000**, *405*, 929–932; b) S. Takaishi, Y. Tobu, H. Kitagawa, A. Goto, T. Shimizu, T. Okubo, T. Mitani, R. Ikeda, *J. Am. Chem. Soc.* **2004**, *126*, 1614–1615. c) S. Takaishi, M. Yamashita, H. Matsuzaki, H. Okamoto, H. Tanaka, S. Kuroda, A. Goto, T. Shimizu, T. Takenobu, Y. Iwasa, *Chem. Euro. J.* **2008**, *14*, 472–477.
- [7] H. Tanino, K. Kobayashi, *J. Phys. Soc. Jpn.* **1983**, *52*, 1446–1456.
- [8] a) R. J. H. Clark, M. L. Franks, W. R. Trumble, *Chem. Phys. Lett.* **1976**, *41*, 287–292. b) R. J. H. Clark, M. Kurmoo, D. N. Mountney, H. Toftlund, *J. Chem. Soc., Dalton Trans.* **1982**, *1982*, 1851–1860; c) R. J. H. Clark, *Chem. Soc. Rev.* **1990**, *19*, 107–131.
- [9] a) M. Tanaka, S. Kurita, T. Kojima, Y. Yamada, *Chem. Phys.* **1984**, *91*, 257–65; b) Y. Wada, T. Mitani, M. Yamashita, T. Koda, *J. Phys. Soc. Jpn.* **1985**, *54*, 3143–3153.
- [10] H. Wolfram, Dissertation 1900, Königberg.
- [11] a) S. Takaishi, M. Takamura, T. Kajiwara, H. Miyasaka, M. Yamashita, M. Iwata, H. Matsuzaki, H. Okamoto, H. Tanaka, S.-i. Kuroda, H. Nishikawa, H. Oshio, K. Kato, M. Takata, *J. Am. Chem. Soc.* **2008**, *130*, 12080–12084; b) S. Kumagai, S. Takaishi, B. K. Breedlove, H. Okamoto, H. Tanaka, S. Kuroda, M. Yamashita, *Chem. Commun.* **2014**, *50*, 8382–8384; c) M. Yamashita, S. Takaishi, *Chem. Commun.* **2010**, *46*, 4438–4448.
- [12] A. Hazell, *Acta Cryst. C*, **1991**, *47*, 962–966.
- [13] a) M. A. Spackman and D. Jayatilaka, *CrystEngComm*, **2009**, *11*, 19–32; b) M. A. Spackman, J. J. McKinnon, *CrystEngComm*, **2002**, *4*, 378–392.
- [14] a) K. Okaniwa, H. Okamoto, T. Mitani, K. Toriumi, M. Yamashita, *J. Phys. Soc. Jpn.* **1991**, *60*, 997–1004.
- [15] a) S. Takaishi, D. Kawakami, M. Yamashita, M. Sasaki, T. Kajiwara, H. Miyasaka, K.-i. Sugiura, Y. Wakabayashi, H. Sawa, H. Matsuzaki, H. Kishida, H. Okamoto, H. Watanabe, H. Tanaka, K. Marumoto, H. Ito, S.-i. Kuroda, *J. Am. Chem. Soc.* **2006**, *128*, 6420–6425. b) S. Takaishi, H. Miyasaka, K. Sugiura, M. Yamashita, H. Matsuzaki, H. Kishida, H. Okamoto, H. Tanaka, K. Marumoto, H. Ito, S.-i. Kuroda, T. Takami, *Angew. Chem. Int. Ed. Engl.* **2004**, *24*, 3171–3175.

Submitted: January 27, 2016

Accepted: January 29, 2016